HEAT AND MASS TRANSFER AND PROPERTIES OF WORKING FLUIDS AND MATERIALS

Convective Heat Transfer Enhancement Inside Tubes Using Inserted Helical Coils[1]

R. K. Ali, M. A. Sharafeldeen, N. S. Berbish, and M. A. Moawed

Benha University, Cairo, Shoubra street, 108, 11689, Egypt
e-mail: Ragabkhalil1971@gmail.com

Abstract—Convective heat transfer was experimentally investigated in tubes with helical coils inserts in turbulent flow regime within Reynolds number range of $14400 \leq \mathrm{Re} \leq 42900$. The present work aims to extend the experimental data available on wire coil inserts to cover wire diameter ratio from 0.044 to 0.133 and coil pitch ratio from 1 to 5. Uniform heat flux was applied to the external surface of the tube and air was selected as fluid. The effects of Reynolds number and wire diameter and coil pitch ratios on the Nusselt number and friction factor were studied. The enhancement efficiency and performance criteria ranges are of (46.9–82.6%) and (100.1–128%) within the investigated range of the different parameters, respectively. Correlations are obtained for the average Nusselt number and friction factor utilizing the present measurements within the investigated range of geometrical parameters and Re.

The aim of augmented heat transfer is to achieve higher heat transfer coefficients and consequently accommodate high heat fluxes to reduce the size and cost of heat exchangers. Enhancement techniques are classified into:

—methods in which the inner surface of the tube is roughened e.g., repeated or helical ribbing, sanding, internal fins or corrugation;

—methods in which a heat transfer promoter e.g., twisted tape, coiled wires, disks or stream lined shapes are inserted into the tubes.

Coiled wire inserts have received a considerable attention because of its practical importance in many industrial applications like oil cooling devices, air preheaters or fire and water tube boilers. The main advantages of helical wire coil inserts in relation to other enhancement techniques are preservation of original plain tube mechanical strength and possibility of installation in an existing smooth tube heat exchanger.

Liu and Sakr [1] introduced a comprehensive review on passive heat transfer enhancements in pipe heat exchangers. They found that variously developed twisted tape inserts are popular researched and used to strengthen the heat transfer efficiency for heat exchangers in laminar flow. The authors observed that limitation studies were performed on the other several passive techniques. However, the other several passive techniques such as coiled wire, ribs, conical nozzle, and conical ring are generally more efficient in the turbulent flow than in the laminar flow. The available pre-

vious studies which have been carried out on wire coils in single-phase flow are summarized in Table 1. The studies on laminar and transition flows are limited [2–7]. Uttarwar and Raja Rao [2] studied seven wires using servotherm oil as test fluid. They found that the increase in friction factor is considerably less than the increase in Nusselt number. Their heat transfer results are affected by the entry region and they did not provide a friction factor correlation.

Inaba et al. [3] introduced an experimental work for the laminar-transition-turbulent flow within a Reynolds number range from 200 to 6000 using water as test fluid. They correlated friction factor and Nusselt number within the investigated ranges. The insertion of wires coils in a smooth tube accelerates significantly the transition to turbulence as shown in García et al. [4]. The transition is produced at Reynolds numbers between 700 and 1000 depending on the wire pitch. Muñoz-Esparza and Sanmiguel-Rojas [5] employed CFD simulation package to investigate the heat transfer and fluid flow performance inside pipe with coiled wire inserts. They found that the friction factor becomes constant in Reynolds number range of 600–850. The effect of the coil pitch on the friction factor has been addressed by performing a parametrical study within the illustrated domain for wire coils. They showed that the increase in coil pitch decreases the friction factor.

Akhavan-Behabadi et al. [6] investigated seven coiled wires with pitches from 12mm to 69 mm, and wire diameters of 2.0 and 3.5 mm and tested for the engine oil. They concluded that wire coil inserts with

---

[1] The article is published in the original.

Table 1. The investigated ranges of available published works on coiled wire inserts

| Autors	Type of investigation	Re	P/d	e/d	Tested fluid
Uttarwar and Raja Rao [2]	Experimental	300–700	0.4–2.62	0.08–0.13	Servotherm oil (Pr = 300−675)
Inaba et al. [3]	Experimental	200–6000	0.3–6.5	0.12–0.19	Water (Pr = 3.9–8.2)
García et al. [4]	Experimental	200–3000	1.25–3.37	0.076	A mixture of 50% water and propylenegly col 50%
Mucoz-Esparza and San-miguel-Rojas [5]	Numerical and experimental	Up to 1000	1.5–4.5	0.074	Propylene–glycol
Akhavan-Behabadi et al. [6]	Experimental	10–1500	7 pitches of 12 −69 mm	Wire diameter 2.0 and 3.5 mm	Oil
García et al. [7]	Experimental	80–90000	1.17–2.68	0.07–0.10	Water and water–propylene glycol mixtures (Pr = 2.8 −150)
Gunes et al. [8]	Experimental	3500–27000	1.0, 2.0, and 3.0	0.0714 è 0.0892	Air (Pr = 0.7)
Gunes et al. [9]	Experimental	4105–26420	1.0–3.0	0.12	Air (Pr = 0.7)
Promvonge [10]	Experimental	5000–25000	0.32–0.42	0.042–0.063	Air (Pr = 0.7)
Sethumadhavan and Raja Rao [11]	Experimental	4000–100000	0.40–2.64	0.08–0.12	Water–glycerol (5.2–32)
Kumar and Judd [12]	Experimental	7000–100000	1.05–5.50	0.11–0.15	Water (Pr = 4.3)
Klaczak [13]	Experimental	1700–20000	0.68–2.88	0.1–0.22	Water (Pr = 2.5–9.0)
Zhang et al. [14]	Experimental	6000–80000	0.35–0.48	0.04–0.09	Air (Pr = 0.7)
Ravigururajan and Bergles [15]	Experimental	5000–25000	0.6–1.12	0.02–0.05	Air (Pr = 0.7)
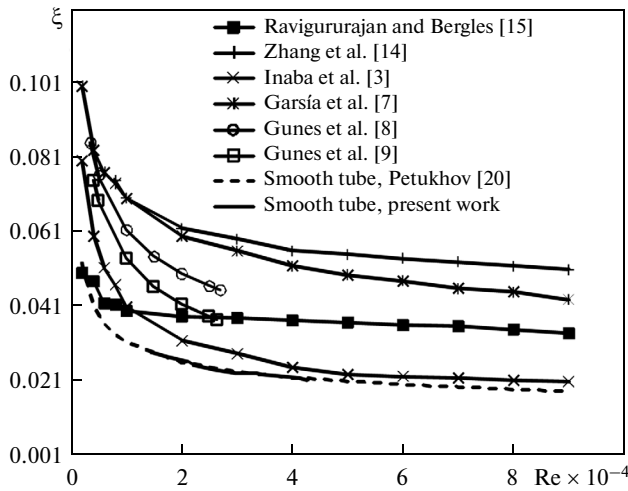
Fig. 1. Comparison of the published friction factor correlations for coiled wire of $P/d = 1.2$ and $e/d = 0.1$.
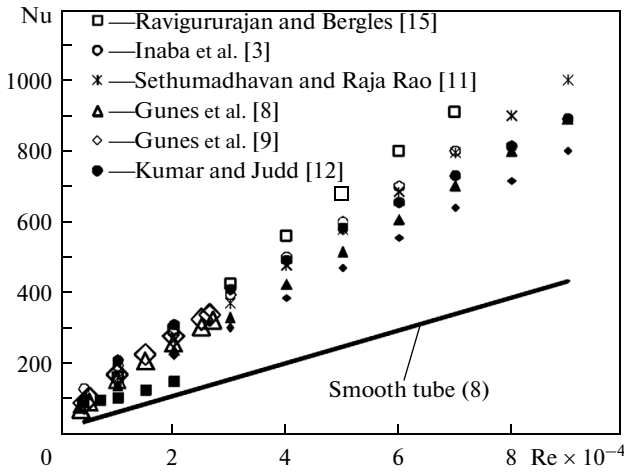

Fig. 2. Comparison of the published Nusselt number correlations for coiled wire of $P/d = 1.2$, $e/d = 0.1$ and $Pr = 6$.
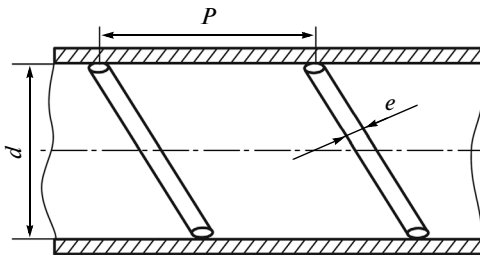

Fig. 3. Sketch of a helical coiled wire fitted inside a smooth tube.

lower wire diameters have better performance, especially at low Reynolds numbers. Also, the increase in the coil pitch made a moderate decrease in performance parameter. The experimental correlations of

Nusselt number and friction factor of the available literature works are shown in Figs. 1 and 2.

García et al. [7] investigated a wide range of Reynolds number for water and propylene glycol mixtures flow. In laminar flow, results show that wire coils behave mainly as a smooth tube. In turbulent flow, wire coils cause a high increase in the pressure drop which depends mainly on coil pitch ratio.

Gunes et al. [8] experimentally investigated coiled wire with equilateral triangular cross section separately from the tube wall by $s = 1$ mm. They showed that as the pitch increases, the vortex shedding frequencies decrease and the maximum amplitudes of pressure fluctuation of vortices produced by coiled wire turbulators occur with small pitches. Gunes et al. [9] introduced an experiments with a constant wire thickness of 6 mm for two different distances ($s = 1$ and 2 mm) at which the coiled wire inserts were placed separately from the tube wall. Their results showed that the Nusselt number and friction factor increase with decreasing pitch ratio and separation distance for coiled wire inserts.

Promvonge [10] investigated the effects of wires with square cross section forming a coil used as a turbulator inside circular tubes. Their results are also compared with those obtained using a typical coiled circular wire. The coiled square wire provides higher heat transfer than the circular one under the same conditions. Also, performance evaluation criteria to assess the real benefits in using both coil wires of the enhanced tube are determined. Sethumadhavan and Raja Rao [11] applied the similarity law approach to interpret the friction and heat transfer results and correlate them in terms of roughness Reynolds number, momentum and transfer roughness functions which is applicable for different types of rough surfaces. Kumar and Judd [12] concluded that coiled wire promoters can be used with advantage for cases where pumping power is not the dominating factor and reduction in weight and size of the equipment is more important. Klaczak [13] introduced a correlation for Nusselt number as a function Reynolds number and wire diameter and coil pitch ratios using water as tested fluid. A significant dispersions among friction factor and Nusselt number correlations are observed as shown in Figs. 1 and 2. The results show differences up to a factor of 2 in the friction factor and Nusselt number. Rabas [16] compiled friction factor data taken from several sources. He stated that there is a marked lack of pressure drop data since many authors do not provide them.

The present paper aims to extend the experimental data available on wire coil inserts. Heat transfer and pressure drop results from nine coiled were investigated. Figure 3 is a sketch of the pipe section with a helical insert with a designation of the basic parameters of the insert and Fig. 3 shows the geometrical range which has been covered in the present work

Table 2. Configurations of the inserted helical coils

Cases	d, mm	P, mm	e, mm	P/d	e/d
Wc2	45	90	2	2	0.044
Wc3	45	90	3	2	0.066
Wc4	45	90	4	2	0.088
Wc5	45	90	5	2	0.111
Wc6	45	45	6	1	0.133
Wc7	45	90	6	2	0.133
Wc8	45	135	6	3	0.133
Wc9	45	180	6	4	0.133
Wc10	45	235	6	5	0.133

compared with those from other published investigations. The configurations of the inserted helical coils used in this investigation are shown in Table 2. A performance evaluation criterion has been used in order to assess the real benefit which wire coil devices offer in turbulent flow. Finally, Nusselt number and friction factor correlations are proposed for turbulent regime in terms of Re and inserts geometry.

EXPERIMENTAL SETUP

The experimental facility employed in the present investigation is shown schematically in Fig. 5. It consists of centrifugal blower, transition section, entrance length, test section, and instrumentations to measure temperature, air flow rate, pressure drop and electrical power input. A centrifugal type air blower driven by an AC motor of 3 hp is used to induce the required flow rate. A transition piece is used to connect the square exit of the blower (60×60 mm) with the circular inlet of the entrance length of 45 mm diameter.

A flexible joint is installed between the exit of blower and the transition section to avoid transferring motor vibration to the test section. The hydrodynamic entry length ranges from 11 to 43 times the hydraulic diameter at Re = 10^4 and 10^5, respectively (Zhi-qing [17]). An entrance section with a circular cross section of 45 mm diameter, 2.5 mm thickness and a length of 1700 mm is applied in the present setup. The air flow rate is controlled using three gate valve installed at the inlet of the entrance section.

The test section is composed of test tube, inserted helical coil, the heating element, insulation layer and end section as shown in Fig. 6, a. The test tube is made of copper with length of 2000 mm, 45 and 50 mm inner and outer diameters, respectively. The air inlet temperature is measured using two thermocouples located far from the test section to avoid the effect of heating section. Thirty six thermocouples of 0.5 mm diameter are installed in the test section and used to measure the temperature along the tube surface. The thermocouples are cemented on the drilled holes at

eighteen axial locations such that a pair of thermocouples is installed in every station. The axial distribution of these thermocouples are shown in Fig. 6b. The helical coil is made of a copper wire with 1, 2, 3, 4 and 6 mm diameter. The helical coils are inserted in the tube with pitches of 20, 40, 60, 80, and 100 mm.

The tube is heated by electrical resistance wire made of nickel chrome of 0.4 mm and 1.55 Ω/m which is wounded uniformly around the test section. The test section is covered by 13 mm thick layer of wool glass thermal insulation as shown in Fig. 6a. Five pressure taps of 12.5 mm diameter are installed at equal distance 500 mm and connected to digital differential manometer to measure the pressure drop across the test section.

The PVC end section is a circular cross section tube with diameter 45 mm, thickness 2.5 mm and length 0.5 m. The end section is used to reduce the axial conduction.

The local velocity of air is measured using digital pitot tube Anemometer across the tube section which is integrated to obtain the average velocity. Tempera-
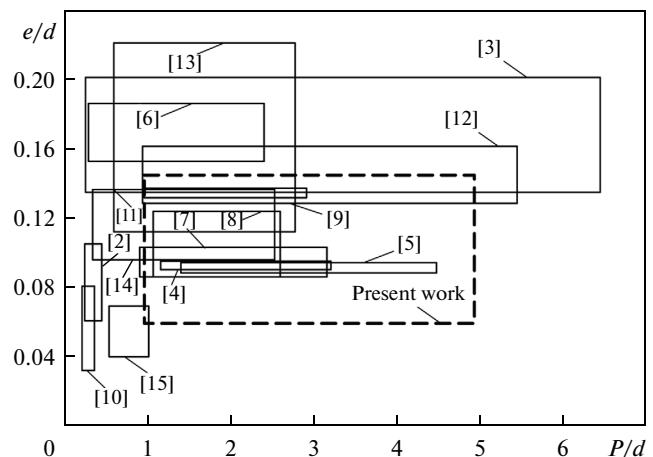
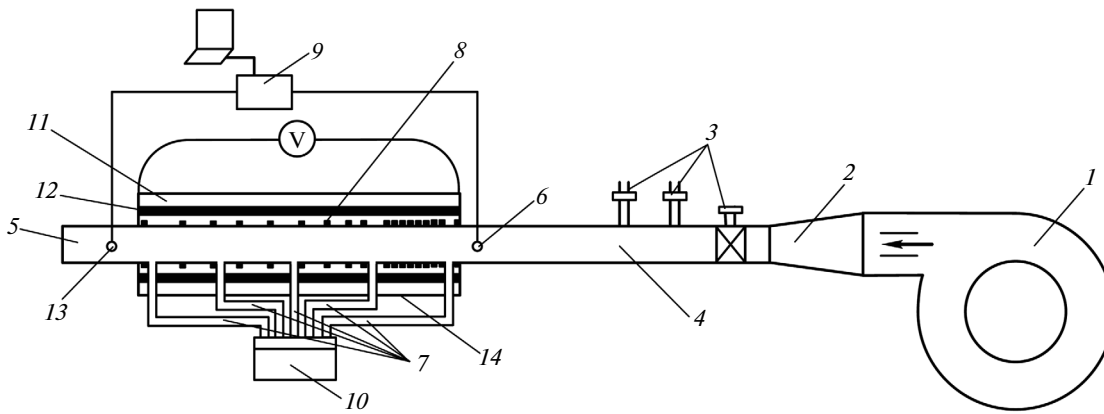**Fig. 4.** Geometrical range of present work in comparison to the available previous studies.

Fig. 5. Schematic diagram of experimental setup. *1*—blower; *2*—transition section; *3*—flow valves; *4*—entrance section; *5*—end section; *6*—inlet thermocouple; *7*—pressure taps; *8*—thermocouples; *9*—data acquisition system; *10*—differential manometer; *11*—thermal insulation; *12*—electrical heaters; *13*—outlet flow thermocouple; *14*—test section
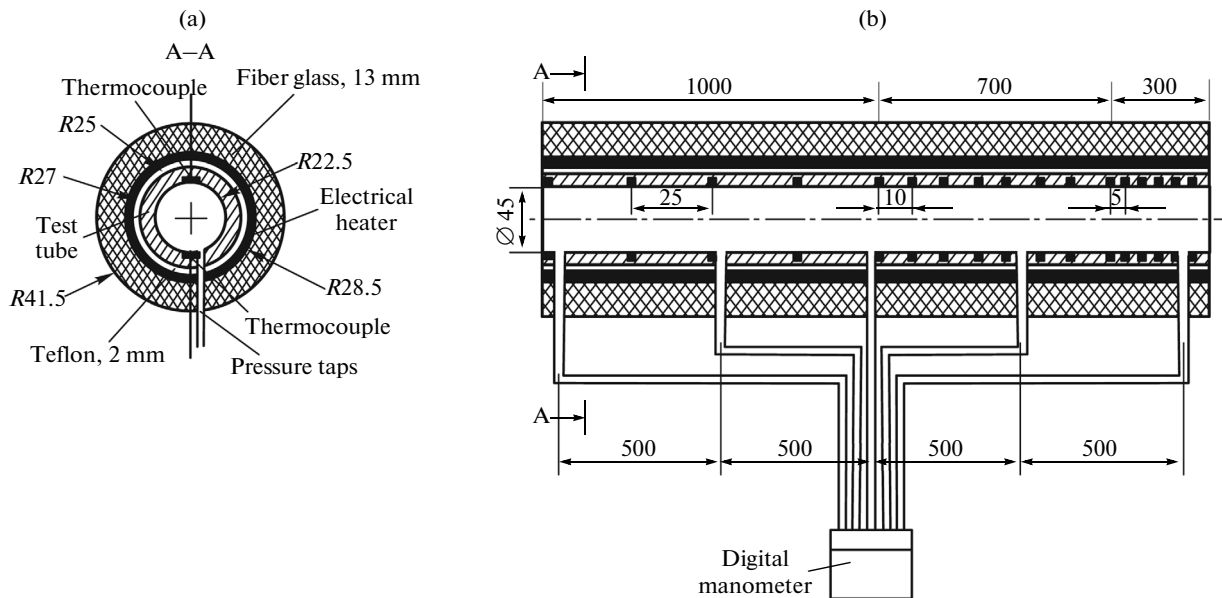

Fig. 6. Cross section A–A (a) and details of the test rig (b).

ture of insulation outer surface is measured by infrared thermometer. Data acquisition system is used to record the thermocouples readings.

EXPERIMENTAL PROCEDURES AND DATA REDUCTION

Before the onset of a data run, the flow rate and power supplied to the heating element are turned on and adjusted for predetermined values. Once the heating element reaches steady state, the element surface temperatures, inlet air temperature, velocity scanning, and voltage applied on the heater are recorded. A series of experiments were carried within the range of Reynolds number from 14400 to 42900. The input

electrical power to the heat sources Q is corrected for conduction loss Q_{loss}:

$$Q = Q_h - Q_{loss}. \qquad (1)$$

The input power to the heater Q_h is regulated with 1 kW AC transformer and can be calculate by the formula

$$Q_h = \frac{V^2}{R}\cos\varphi,$$

where V—applied volt; R—electrical resistance heater; $\cos\varphi$—the AC power factor is assumed to be 0.95.

The conduction loss across the asbestos layers is estimated from

$$Q_h = \frac{2\pi\lambda L(t_{c1} - t_{c2})}{\ln\dfrac{d_1}{d_2}}, \qquad (2)$$

where t_1 and t_2—the average temperature of insulation inner and outer surfaces; d_1 and d_2—the outer and inner diameters of the thermal insulation; λ—asbestos thermal conductivity; L—the length of the heated section.

In all experiments, the conduction loss does not exceed 10% of the input electrical power.

The results are presented in terms of the local convective heat transfer coefficient $\alpha(x)$. It is described as follows

$$\alpha(x) = \frac{q_c}{t_{SA} - \bar{t}_f}, \qquad (3)$$

where t_{SA} and $\bar{t}_f$—the temperatures of tube surface and fluid at a specific location x.

The applied heat flux q_c on the internal surface of the tube is calculated from

$$q_c = Q/F,$$

where F—the internal surface area of the heated section.

The average heat transfer coefficient $\bar{\alpha}$ can be calculated from the following relation:

$$\bar{\alpha} = \frac{1}{L}\int_{L_T}^{L} \alpha(x)\mathrm{d}x, \qquad (4)$$

where L_T is the thermal fully developed length.

The average value Nusselt was defined as

$$\overline{Nu} = \frac{\bar{\alpha}d}{\lambda_f}, \qquad (5)$$

where λ_f—air thermal conductivity.

Reynolds number is calculated using average velocity $\bar{w}$ as

$$Re = \frac{\rho_f \bar{w} d}{\mu_f}, \qquad (6)$$

where ρ_f and μ_f—air density and dynamic coefficient viscosity.

The average velocity $\bar{w} = \dfrac{4}{\pi d^2}\int_{0}^{d/2} 2\pi r w(r)\mathrm{d}r$ is calculated from integration the local velocity obtained from velocity scanning process using digital pitot tube anemometer.

The friction factor is calculated from the following relation:

$$\xi = \frac{2\Delta p d/L}{\rho \bar{w}^2}, \qquad (7)$$

where Δp—pressure drop across the test section.

The uncertainty in Nusselt number and friction factor is estimated using the differential approximation presented by El-Shazly [18]. The minimum uncertainties of Nusselt number and friction factor are found at high flow rate as 2.6 and 2.5% respectively. The maximum uncertainty in $\overline{Nu}$ is of 4.6% at lower Reynolds number. These values are based on the assumption of negligible uncertainty in the relevant fluid properties. Experimental runs were carried out to investigate the thermal performance of turbulent flow in tube with inserted helical coils with wire diameter ratio of $0.044 \leq e/d \leq 0.133$ and coil pitch ratio of $1 \leq P/d \leq 5$ over a range of Reynolds number $14400 \leq Re \leq 42900$.

RESULTS AND DISCUSSIONS

Firstly, the obtained experimental results of Nusselt number for plain tube are compared with the results obtained from the well-known steady state flow in circular plain tubes Dittus and Boelter equation cited in Incropera and Dewitt [19]:

$$Nu = 0.023\,Re^{0.8}\,Pr^{0.4}. \qquad (8)$$

Also the obtained results for friction factor in turbulent flow are compared with the correlation of Petukhov [20]

$$\xi = (0.79\ln Re - 1.64)^{-2}. \qquad (9)$$

Tables 3 presents a comparison of the experimental data of Nusselt number and friction factor for smooth tube. As seen in Table 3, good agreement between the present experimental results of the smooth tube and the previous correlations is obtained. These results reveal the accuracy of the experimental set up and the used measurement techniques.

Enhancement efficiency and performance criteria are applied to evaluate inserting of wire coil inside tubes. Enhancement efficiency η, based on the same mass flow in smooth and enhanced tubes with wire helical coil is calculated as

$$\eta = \frac{Nu_c/Nu_0}{\xi_c/\xi_0}, \qquad (10)$$

where Nu_c, ξ_c—Nusselt number and friction factor for tubes with wire helical coil; Nu_0, ξ_0—Nusselt number and friction factor for smooth tube.

The performance criteria is expressed as the ratio of heat transfer coefficient of the enhanced tubes with wire helical coil and that of plain tubes for the same pumping power as introduced by Webb [21], Webb and Eckert [22] and Fan et al. [23]

$$\psi = \frac{Nu_c/Nu_0}{(\xi_c/\xi_0)^{1/3}}. \qquad (11)$$

The variation of enhancement efficiency with Reynolds number for different wire diameter and coil pitch ratios are presented in Figs. 7 and 8. It is obvious that enhancement efficiency $\eta < 1$ and tends to decrease with increasing wire diameter ratio and

Table 3. Comparison of the experimental data of Nusselt number and friction factor for smooth tube

Re	Nusselt number data			Friction factor data		
	Present experimental measurements	Dittus and Boelter Eq. (8)	Relative error, %	Present experimental measurements	Petukhov [20], Eq. (9)	Relative error, %
14400	41.7	42.4	1.56	0.029	0.029	0.68
17500	48.5	49.4	1.88	0.028	0.027	1.27
21100	56.5	57.6	1.91	0.026	0.026	0.45
22100	59.8	59.6	0.42	0.026	0.026	1.34
26000	65.5	68.0	3.75	0.024	0.025	2.69
29900	73.0	75.9	3.88	0.023	0.024	2.52
33750	83.5	83.6	0.16	0.023	0.023	0.76
34600	85.3	85.5	0.18	0.023	0.023	1.43
41400	96.2	98.5	2.41	0.022	0.022	0.33
42900	101.4	101.4	0.07	0.021	0.022	2.43

decreasing the coil pitch ratio over the investigated Reynolds number range.

The higher turbulence level accompanied with the induced swirl flow, coil roughness elements, and
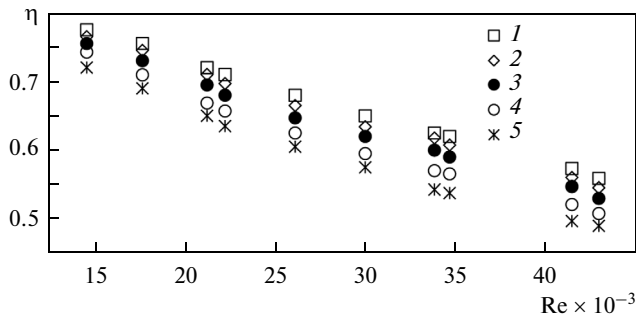

Fig. 7. Enhancement efficiency versus Reynolds number for different wire diameter ratios at $P/d = 2$. Diameter ratio e/d: 1—0.044; 2—0.066; 3—0.088; 4—0.111; 5—0.133
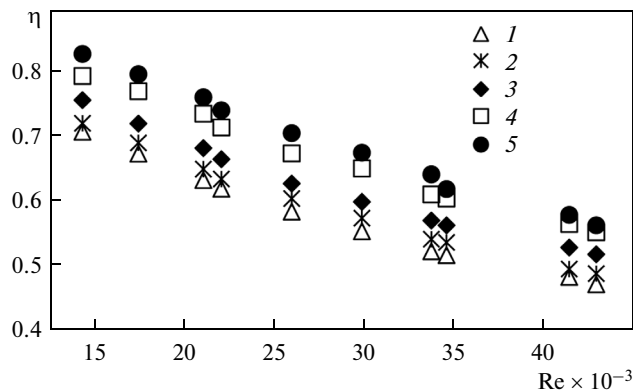

Fig. 8. Enhancement efficiency versus Reynolds number for different coil pitch ratios at $e/d = 0.133$. Marker numbers correspond to the relative pitch P/d.

sequential separation reattachment mechanism produces an increase in friction factor higher than the enhancement in Nusselt number.

Enhancement efficiency is decreased to 71−77% at Re = 14400 and 50−58% at Re = 42900 for $0.044 \leq e/d \leq 0.133$ at $P/d = 2$ as illustrated in Fig. 7. The highest enhancement efficiency of (55−77%) is noticed for $e/d = 0.044$ over $14400 \leq Re \leq 42900$.

The enhancement efficiency is decreased to 69−83% at Re = 14400 and 47−57% at Re = 42900 for $1 \leq P/d \leq 5$ at $e/d = 0.133$ as shown in Fig. 8. Coil pitch ratio of $P/d = 5$ presents the highest enhancement efficiency of (83%) over $14400 \leq Re \leq 42900$.

Figures 9 and 10 illustrate the performance criteria versus Reynolds number for different wire diameter and coil pitch ratios, respectively. From Figs. 9 and 10, it can be seen that performance criteria $\psi > 1$ and increases with increasing wire diameter ratio and decreasing the coil pitch ratio over the investigated Reynolds number range.

From Figs. 9 and 10 it is clear that inserted wire coils are attractive since higher heat transfer rate is conducted for the same pumping power. The increase in the performance criteria for $0.044 < e/d \leq 0.133$ has a range of (118−127%) at Re = 14400 and (101−104%) at Re = 42900 for $P/d = 2$ as shown in Fig. 9. Performance criteria ratio is observed to be highest for $e/d = 0.133$ over Reynolds number range of (104−127%) due to the higher level of turbulence.

The increase in the performance criteria for $1 \leq P/d \leq 5$ has a range of 124−128% at Re = 14900 and 102−105% at Re = 42900 for $e/d = 0.133$ as shown in Fig. 10. Performance criteria ratio is observed to be highest for $P/d = 1$ over all Reynolds number with range of 105−128%.

Correlations of Nusselt number and friction factor for enhanced tubes with coiled wire were obtained as a
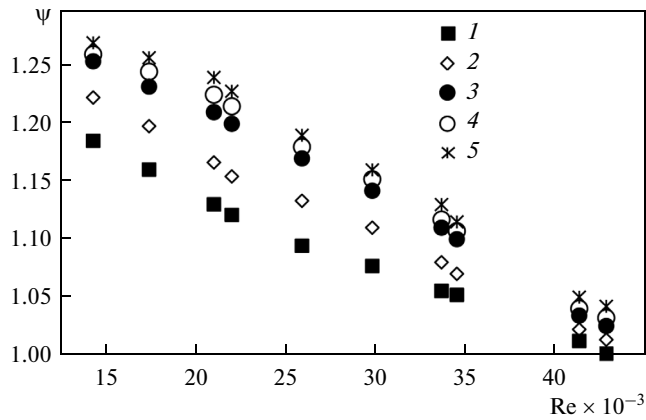
Fig. 9. Performance criteria ψ versus Reynolds number for wire diameter ratios at $P/d = 2$. Notation see Fig. 7.
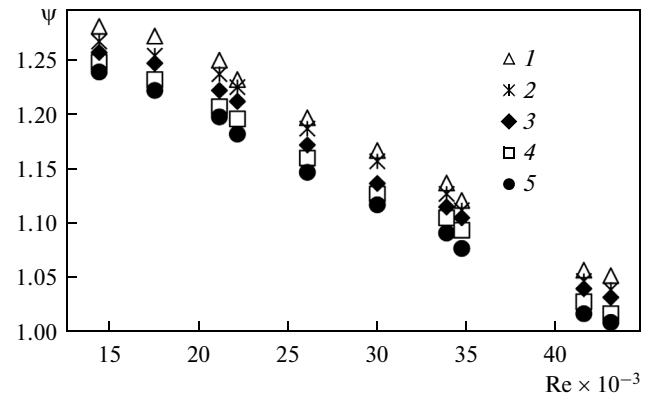

Fig. 10. Performance criteria versus Reynolds number for different coil pitch ratios at $e/d = 0.133$. Marker numbers correspond to the relative pitch P/d.
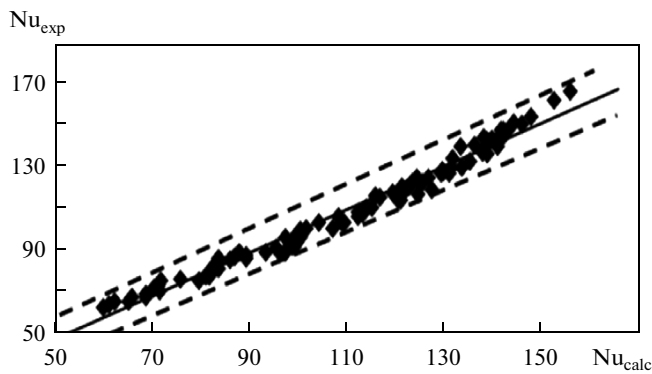

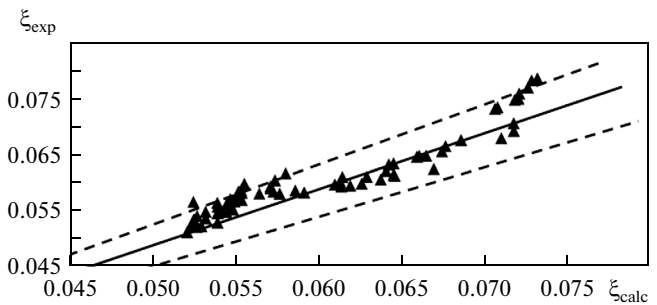**Fig. 11.** Experimental versus correlated data for Nusselt number.

Fig. 12. Experimental versus correlated data for friction factor.

function of wire diameter and coil pitch ratios and Reynolds number as follows

$$\mathrm{Nu_c} = 0.117\,\mathrm{Re}^{0.7}(e/d)^{0.104}(P/d)^{-0.106}; \quad (12)$$

$$\xi_c = 0.3251\,\mathrm{Re}^{-0.101}(e/d)^{0.196}(P/d)^{-0.211}. \quad (13)$$

The correlations are valid for range $0.044 \le e/d \le 0.133$, $1 \le P/d \le 5$, $14400 \le \mathrm{Re} \le 42900$ and $\mathrm{Pr} \approx 0.7$.

Figures 11 and 12 show the correlated versus the experimental data for the Nusselt number and friction factor within the investigated ranges with maximum deviation $\pm 5\%$ for Nusselt number and $\pm 6\%$ for friction factor.

CONCLUSION

1. Turbulence and fluid mixing in tube caused by inserted helical coil is largely responsible for enhanced rate of heat transfer and higher pressure drop.

2. The wire diameter and coil pitch ratios have a noticeable effect on both Nusselt number friction fac-

tor in the coiled tube. The higher values of Nusselt number and friction factor are obtained at higher values of wire diameter ratio and small values of coil pitch ratio.

3. The enhancement efficiency range is of 46.9–82.6% for all studied cases within $0.044 \le e/d \le 0.133$, $1 \le P/d \le 5$ and $14400 \le \mathrm{Re} \le 42900$.

4. Inserted wire coils are attractive since higher heat transfer rate is conducted for the same pumping power. The performance criterion range is of (101–128%) for all studied cases within $0.044 \le e/d \le 0.133$, $1 \le P/d \le 5$ and $14400 \le \mathrm{Re} \le 42900$.

5. Correlations are obtained for the average Nusselt number and friction factor utilizing the present measurements within $0.044 \le e/d \le 0.133$, $1 \le P/d \le 5$ and $14400 \le \mathrm{Re} \le 42900$ for $\mathrm{Pr} \approx 0.7$.

REFERENCES

1. S. Liu and M. Sakr, "A comprehensive review on passive heat transfer enhancements in pipe exchangers," Renew and Sustain. Energy Rev. **19**, 64–81 (2013).

2. S. B. Uttarwar and M. Rao Raja, "Augmentation of laminar flow heat transfer in tubes by means of wire coil inserts," Trans. ASME **107**, 930−935 (1985).

3. H. Inaba, K. Ozaki, and S. Kanakoa, "A fundamental study of heat transfer enhancement and flow-drag reduction in tubes by means of wire coil insert," Jpn. Soc. Mech. Eng. **60**, 240−247 (1994).

4. A. García, J. P. Solano, P. G. Vicente, and A. Viedma, "Flow pattern assessment in tubes with wire coil inserts in laminar and transition regimes," Int. J. Heat Fluid Flow **28**, 516−525 (2007).

5. D. Muñoz-Esparza and E. Sanmiguel-Rojas, "Numerical simulations of the laminar flow in pipes with wire coil inserts," Comput. Fluids **44**, 169−177 (2011).

6. M. A. Akhavan-Behabadi, R. Kumar, M. R. Salimpour, and R. Azimi, "Pressure drop and heat transfer augmentation due to coiled wire inserts during laminar flow of oil inside a horizontal tube," Int. J. Therm. Sci. **49**, 373−381 (2010).

7. A. García, P. G. Vicente, and A. Viedma, "Experimental study of heat transfer enhancement with wire coil inserts in laminar-transition-turbulent regimes at different Prandtl numbers," Int. J. Heat Mass Transfer **48**, 4640−4651 (2005).

8. S. Gunes, V. Ozceyhan, and O. Buyukalaca, "Heat transfer enhancement in a tube with equilateral triangle cross sectioned coiled wire inserts," Exp. Therm. Fluid Sci. **34**, 684−691 (2010).

9. S. Gunes, V. Ozceyhan, and O. Buyukalaca, "The experimental investigation of heat transfer and pressure drop in a tube with coiled wire inserts placed separately from the tube wall," Appl. Therm. Eng. **30**, 1719−1725 (2010).

10. P. Promvonge, "Thermal performance in circular tube fitted with coiled square wires," Energy Convers. Manag. **49**, 980−987 (2010).

11. R. Sethumadhavan and M. R. Rao, "Turbulent flow heat transfer and fluid friction in helical-wire-coil-inserted tubes," Int. J. Heat Mass Transfer **26**, 1833−1845 (2008).

12. P. Kumar and R. L. Judd, "Heat transfer with coiled wire turbulence promoters," Can. J. Chem. Eng. **48**, 378−383 (1970).

13. A. Klaczak, "Heat transfer in tubes with spiral and helical turbulators," J. Heat Transfer **95**, 557−559 (1973).

14. Y. F. Zhang, F. Y. Li, and Z. M. Liang, "Heat transfer in spiral coil-inserted tubes and its application," Adv. Heat Transfer Augment. Mixed Convect., ASME HTD **169**, 31−36 (1991).

15. T. S. Ravigururajan and A. E. Bergles, "Development and verification of general correlations for pressure drop and heat transfer in single-phase turbulent flow in enhanced tubes," Exp. Therm. and Fluid Sci. **13**, 55−70 (1996).

16. T. J. Rabas, "Prediction methods for single phase turbulent flow inside tubes with wire-coil inserts," Optim. Des. Therm. Syst. Compon., ASME HTD **279**, 91−97 (1994).

17. W. Zhi-qing, "Study on correction coefficients of laminar and turbulent entrance region effects in round pipes," Appl. Math. Mech. **3**, 433−441 (1982).

18. K. M. El-Shazly, *Effect of Darcian and Non-Darcian Natural Convection on the Effective Thermal Conductivity of a Porous Medium* (Faculty of Engineering, Cairo University, 1991).

19. F. Incropera and P. D. Dewitt, *Introduction to Heat Transfer* (Wiley, New York, 1996).

20. B. S. Petukhov, *Heat Transfer in Turbulent Pipe Flow with Variable Physical Properties* (Academic, New York, 1970).

21. R. L. Webb, "Performance evaluation criteria for use of enhanced heat transfer surfaces in heat exchanger design," Int. J. Heat Mass Transfer **24**, 715−726 (1981).

22. R. L. Webb and E. R. G. Eckert, "Application of rough surface to heat exchange design," Int. J. Heat Mass Transfer **15**, 1647−1658 (1972).

23. J. F. Fan, W. K. Ding, J. F. Zhang, Y. L. He, and W. Q. Tao, "A performance evaluation plot of enhanced heat transfer techniques oriented for energy-saving," Int. J. Heat Mass Transfer **52** (2), 33−34 (2009).